

Planning load-effective dynamic motions of highly articulated human model for generic tasks

Joo H. Kim^{*,†}, Jingzhou Yang[‡] and Karim Abdel-Malek[†]

[†]*U.S. Army Virtual Soldier Research Program, Center for Computer-Aided Design, The University of Iowa, Iowa City, IA 52242, USA.*

[‡]*Department of Mechanical Engineering, Texas Tech University, Lubbock, TX 79409, USA.*

(Received in Final Form: August 11, 2008. First published online: October 20, 2008)

SUMMARY

The robotic motion planning criteria has evolved from kinematics to dynamics in recent years. Many research achievements have been made in dynamic motion planning, but the externally applied loads are usually limited to the gravity force. Due to the increasing demand for generic tasks, the motion should be generated for various functions such as pulling, pushing, twisting, and bending. In this paper, a comprehensive form of equations of motion, which includes the general external loads applied at any point of branched tree structures, is implemented. An optimization-based algorithm is then developed to generate load-effective motions of redundant tree-structured systems for generic tasks. A highly articulated dual-arm human model is used to generate different effective motions to sustain different external load magnitudes. The results also provide a new scientific insight of human motion.

KEYWORDS: Motion planning; Equation of motion; Load-effective; Optimization; Redundant; General external load; Tree structure.

1. Introduction

One of the major applications of robotic technologies lies in improving human life by utilizing robots in jobs that are hazardous, difficult, or undesirable for humans. Recently, dependency on robots for the tasks associated with these jobs has been growing very rapidly. The robots are also used for providing services in the public and private sectors. Broadening the applications of robots usually requires adding functions and increasing accuracies and capabilities. One way to achieve this is to increase the mobility of robots such that multiple alternate motions exist for performing an assigned task. In other words, higher-level robots must possess redundancy. The redundancy of robots will provide higher flexibility, dexterity, manipulability, and controllability. Good examples of these higher-level robots are seen in the recent developments of humanoids, bio-inspired robots, and space robots.

Despite great achievements in the research on motion planning, the methodologies in the current literature do not extensively address the exertion of general external loads (forces and moments) other than gravity. Nonredundant

systems have only one possible configuration at a time, and whether a task can be accomplished or not is determined by that configuration; redundant systems can possess an infinite number of configurations at a time, and successful task accomplishment depends on the proper choice of configurations. Thus, it is important to investigate appropriate methods of generating redundant system motions that provide the desired results.

While most of the motion planning methods in the literature had been based on spatial kinematics,^{1,2} the recent research on dynamics-based motion planning has shown huge achievement. This is because motion planning based on kinematic constraints alone is not always satisfactory in real execution. Since the planned motions are supposed to be executed in a real physical environment, the selection of the motion should incorporate the dynamic constraints. Incorporating the dynamics in motion generation is facilitated and widened especially by the recent developments of efficient dynamics algorithms. Many numerical strategies (mostly recursive) have been invented to improve the efficiency of the forward and inverse dynamics. Some examples are: system coordinate partitioning method,^{3,4} spatial operator factorizations of mass matrix,⁵ symbolic decomposition of the inertia matrix by Gaussian elimination,⁶ low-order parallelization,^{7,8} reduced-dimension formulations using pseudo-inverse Jacobian,⁹ state space form using stable feedback inverse systems,¹⁰ and mass matrix inversion based on Lie group and Fixman's theorem.¹¹

The redundancy of a system requires the selection of the best configuration among many admissible ones, and thus the majority of the studies used optimization methods. Some studies used gradient-based numerical optimization; some derived the pseudo-inverse analytically from optimization; and others used a mixture of the pseudo-inverse and numerical optimization.¹² Due to the closed form and low-cost computations, the pseudo-inverse, or generalized inverse, of the Jacobian matrices are popular tools for resolution of kinematic redundancy. Most of the Jacobian pseudo-inverse matrices in literature were derived from minimum kinetic energy criteria.^{13,14} Nedungadi and Kazerounian¹⁵ optimized weighted torque and kinetic energy by the method of calculus of variation combined with the pseudo-Jacobian matrix, where local and global optimal forms were demonstrated for comparison. Chung *et al.*¹⁶ introduced a Jacobian pseudo-inverse that represents a minimization of

* Corresponding author. E-mail: jookim@engineering.uiowa.edu

the pseudo-elastic potential energy due to actuator stiffness. A control scheme for redundant manipulators is developed by optimizing a norm of actuator torques using the weighted generalized inverses of the Jacobian matrix.¹⁷ In this method, the equation of motion that includes the contact forces due to target impedance was used, where the contact is modeled with inertia, damping, and stiffness.

Many methods on redundant system motion planning have been developed based on gradient-based numerical optimization. Shiller and Dubowsky^{18,19} developed algorithms of local and global time-optimal motion planning for manipulators with obstacle avoidance, where the robot dynamics, actuator constraints, and singularities are considered. Also, various approximate forms of energy consumption or effort were minimized while the dynamic equations of motion were used either to derive the cost function or to impose dynamic constraints.^{20–22} Bobrow *et al.*²³ developed the dynamics and optimal control of manipulators using rigorous mathematics, in which the recursive robot dynamics are represented based on Lie groups and Lie algebras. They proposed the linear quadratic algorithm that is numerically stable and efficient for optimal motion planning with multibody dynamics. On the other hand, more exact forms of energy consumption of electric motors and hydraulic actuators were derived by combining the equations of motion, and these were minimized for optimal motion planning subject to dynamic constraints.^{24,25} The equations of motion used in these studies include the inertia, Coriolis, centrifugal, and gravity terms, and thus the external loads are limited to the weights of the links or the objects at the end-effector. In all the aforementioned studies, however, the general form of external loads such as pushing/pulling forces and bending/twisting moments are not incorporated in the dynamic motion planning application.

Some researchers investigated the methods of determining manipulator configurations to sustain general external loads (wrench) for static postures or quasi-static motions.^{26–28} Papadopoulos and Gonthier^{27,28} developed a method of determining the base position and configuration of the manipulator that guarantees the execution of a large-force task under limited actuator torques. The maximum normalized torque to generate the manipulator postures is minimized subject to general external loads and gravity in static and quasi-static states, while the dynamic effects of the accelerations and velocities are not taken into account. Although the quasi-static evaluation of actuator torques gives reasonable approximate values for manipulators with relatively small link masses and low velocities, the inaccuracy of the calculation increases as the link masses, the velocities, or the accelerations of the motion become larger (e.g., manipulators used for construction) due to the significant contributions of the inertia forces.

In recent years, many studies on human dynamics and motion planning have been presented. McLean *et al.*²⁹ used a variable step fourth-order Runge–Kutta method to solve the forward dynamics problem of the human knee. The muscle stimulation patterns as well as the initial conditions are given as inputs, where the muscle forces are calculated from the muscle stimulation via a muscle activation model and measured data. The resulting lower-body motions were

reliable compared with the experimental measurement. Blajer and Czaplicki³⁰ proposed a compact and systematic way of human multibody dynamics that does not involve matrix inversion, which is thus suited for both symbolic and computational implementations. Hirashima *et al.*³¹ used the Newton–Euler dynamics for human model with prescribed motions, where some simple motions of shoulder, elbow, and wrist joints are given as inputs. As for predictive human motion simulation, many optimization-based methodologies have been shown to be valuable tools due to the high redundancy of human model.^{32–35} This is based on the underlying assumption that a human moves in a way that minimizes a cost function (e.g., energy consumption) subject to several constraints. However, the implementation of general external loads is not considered explicitly in literature for the human motion problem. For realistic physics-based human motion planning, it is essential to consider all components of dynamics so that the task categories should be extended from simple lifting and moving (against gravity) to generic tasks such as pulling, pushing, and twisting. The objectives and contribution of this research are summarized as follows:

1. A general form of dynamics will be derived for branched tree structures. The equations of motion for robotic systems are well known and have been widely used in literature for a long time, and the external contact forces are implemented in some control-based articles.¹⁷ However, in addition to the interaction with external contacts, exertion of various general loads such as pulling forces and twisting moments are usually required. So far, the comprehensive form of dynamics that includes inertia, Coriolis, centrifugal, gravity, and general external loads applied at any point of interest on a tree-structured system has not been explicitly treated in literature. Although various formulations for the dynamics of tree structure were developed, each is based on its own kinematic representation without explicit terms of general external loads.^{36–39} Also, the dynamic contribution of the connection link is not rigorously formulated. In this paper, the dynamics of tree-structured systems is modeled within the framework of the proposed approach, i.e., based on the Denavit–Hartenberg (DH) representation method^{40,41} and generalized coordinates. The complete form of the equations of motion will be used as a critical module for motion planning.
2. The methodology of planning load-effective motions of tree-structured redundant systems will be proposed. We define the load-effective motions as the generated motions that guarantee the execution of a task with given general external loads of a broad range of magnitudes. As seen earlier, although many authors have treated the gravity forces (weights), motions with external loads other than the gravity have not been extensively addressed in the literature. By implementing the comprehensive dynamics, it is possible to generate optimal motions in which the general external loads are incorporated. A dual-arm human model with high degrees of freedom (DOFs) will be used to generate realistic human motions. Different human motions associated with different magnitudes

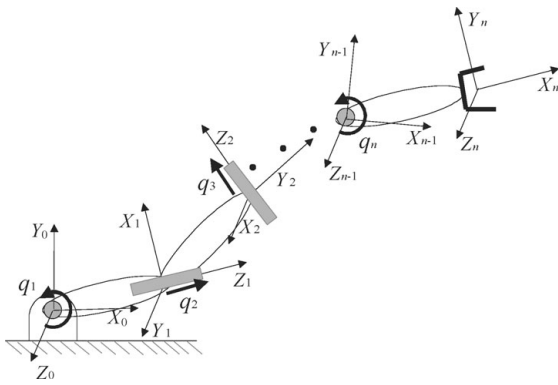


Fig. 1. An n -DOF open-loop kinematic chain.

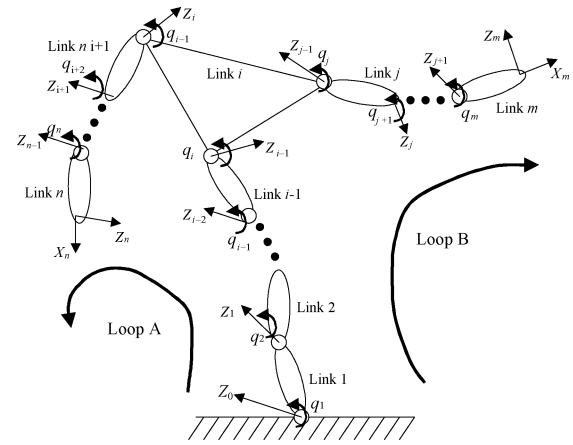


Fig. 2. A tree-structured kinematic chain.

of external load will demonstrate how humans react effectively to perform a task.

In the following sections, the DH kinematic modeling and the comprehensive form of dynamics of tree-structured chains are briefly described. Next, the structure and components of the optimal motion planning problem are presented in detail. Finally, examples for a tree-structured human model are illustrated and discussed.

2. Kinematic and Dynamic Modeling

Given an open-loop kinematic chain (Fig. 1), the transform from frame $\{i\}$ to frame $\{i - 1\}$ can be represented by the homogeneous transformation matrix ${}^{i-1}\mathbf{T}_i(q_i)$ and DH notation, which describes the configuration of a kinematic chain.^{40,41} q_i is the joint variable of ${}^{i-1}\mathbf{T}_i$, and the set of joint variables (or generalized coordinates) $\mathbf{q} = [q_1, \dots, q_n]^T \in \mathbf{R}^n$ uniquely determine the configuration of a kinematic chain system with n DOFs.

As for the kinematic modeling method of tree-structured systems (Fig. 2) using DH representation, the numbering method is the same as a regular serial chain for one loop (loop A, for example). For the other loop (B), the link that is attached to the connection link (link i in Fig. 2) can be given any arbitrary number j , as long as it is greater than

or equal to the last link number of loop A plus two, i.e., $j \geq n + 2$. Then the numbering system of the joints and the local coordinate frames follow the usual convention. Note, however, that since there are three joints at the connection link, different transformation matrices are assigned to each loop. For loop A, the usual transformation matrix ${}^{i-1}\mathbf{T}_i$ is used to relate the local coordinate frames $\{i - 1\}$ and $\{i\}$. To relate the local coordinate frames $\{i - 1\}$ and $\{j - 1\}$ for loop B, another transformation matrix ${}^{i-1}\mathbf{T}_{j-1}$ should be constructed. Since the local frames $\{i\}$ and $\{j - 1\}$ are attached to the connection link, whereas the local frame $\{i - 1\}$ is attached to the link $\{i - 1\}$, the transformation matrix ${}^{i-1}\mathbf{T}_{j-1}$ for loop B is also a function of the i th joint variable (${}^{i-1}\mathbf{T}_{j-1} = {}^{i-1}\mathbf{T}_{j-1}(q_i)$). Whenever there are more than two branches connected with the connection link, a similar process can be used.

Human body is a typical example of tree-structured systems with multiple limbs. The 30-DOF SantosTM human model of a torso, right arm, and left arm is shown in Fig. 3. Using the DH notation, the global Cartesian position vectors \mathbf{x}_R and \mathbf{x}_L of the right-arm and left-arm end-effectors,

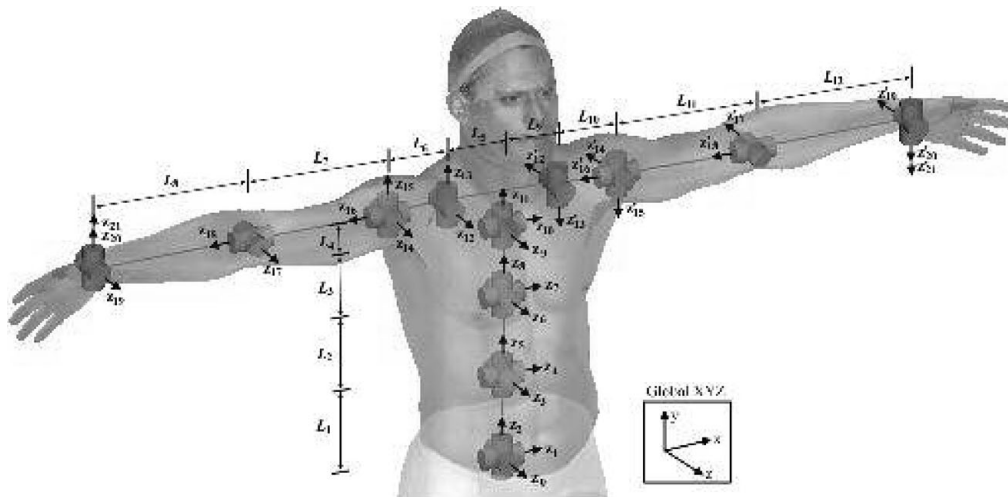


Fig. 3. A dual-arm human model.

respectively, can be calculated.

$$\begin{aligned} \mathbf{x}_R(\mathbf{q}) &= (\mathbf{T}_{\text{torso}})^{11} \mathbf{T}_{12} \left(\prod_{i=13}^{21} {}^{i-1} \mathbf{T}_i \right) \mathbf{x}_{Rn}; \\ \mathbf{x}_L(\mathbf{q}) &= (\mathbf{T}_{\text{torso}})^{11} \mathbf{T}_{22} \left(\prod_{i=23}^{31} {}^{i-1} \mathbf{T}_i \right) \mathbf{x}_{Ln}; \\ \mathbf{T}_{\text{torso}} &= \prod_{i=1}^{11} {}^{i-1} \mathbf{T}_i \end{aligned} \quad (1)$$

where \mathbf{x}_{Rn} and \mathbf{x}_{Ln} are the 4×1 local frame position vectors for the right-arm and left-arm end-effectors, respectively. $\mathbf{T}_{\text{torso}}$ is the transformation matrix of the last local coordinate frame of the torso with respect to the global coordinate frame. ${}^{11} \mathbf{T}_{12}$ and ${}^{11} \mathbf{T}_{22}$ are the transformation matrices for the first local coordinate frame of the right arm and the left arm, respectively, in terms of the last local coordinate frame of the torso. $\prod_{i=13}^{21} {}^{i-1} \mathbf{T}_i$ and $\prod_{i=23}^{31} {}^{i-1} \mathbf{T}_i$ are the transformation matrices for the last local coordinate frame of the right arm and the left arm, respectively, in terms of the first local coordinate frame of the limb.

To generate the motions where the externally applied forces and moments are taken into account, it is essential to formulate a comprehensive expression of the equations of motion that govern the dynamics of open-loop kinematic chains. Consider the case where a general form of external loads (force and moment) $[\mathbf{F}_k^T \ \mathbf{M}_k^T]^T$ is applied to the point at ${}^k \mathbf{r}_k$ location of link k . The Lagrangian equation of motion for a general open-loop kinematic chain with several external loads is as follows³⁵:

$$\begin{aligned} \boldsymbol{\tau} &= \mathbf{M}(\mathbf{q})\ddot{\mathbf{q}} + \mathbf{V}(\mathbf{q}, \dot{\mathbf{q}}) \\ &+ \sum_i \mathbf{J}_i^T m_i \mathbf{g} + \sum_k \mathbf{J}_k^T \begin{bmatrix} -\mathbf{F}_k \\ -\mathbf{M}_k \end{bmatrix} + \mathbf{T}(\mathbf{q}, \dot{\mathbf{q}}) \end{aligned} \quad (2)$$

where $\boldsymbol{\tau} = [\tau_1, \tau_2, \dots, \tau_n]^T$ is the actuator torque vector, $\mathbf{M}(\mathbf{q})$ is the generalized mass-inertia matrix, $\mathbf{V}(\mathbf{q}, \dot{\mathbf{q}})$ is the Coriolis and centrifugal force vector, $\sum \mathbf{J}_i^T m_i \mathbf{g}$ is the joint torque vector due to gravity, \mathbf{J}_i is the Jacobian matrix of the position vector for the center of mass of i th link, and \mathbf{J}_k is the augmented Jacobian matrix of the position vector ${}^k \mathbf{r}_k$ with respect to $\{k\}$ local frame. $\mathbf{T}(\mathbf{q}, \dot{\mathbf{q}})$ is the torque vector due to the joint stiffness and the dissipative forces such as viscous damping and Coulomb friction.

Equation (2) is derived for a single-loop kinematic chain where the first joint is rigidly attached to the global reference frame. To apply the equations of motion module that is coded for single-loop chains to tree structures, consider a tree-structured system with three branches (Fig. 2) under a set of forces and moments. This tree structure is composed of three local branch chains, C_1 , C_2 , and C_3 . The branch chain C_1 is composed of links from link 1 to link i , C_2 from link $i + 1$ to link n , and C_3 from link j to link m .

The Lagrangian function of the whole system is a scalar quantity and is thus calculated as the summation of the Lagrangian function L of each branch. Therefore, the Lagrange's equation of motion for the tree structure is written as the summation of the actuator torque vector at each branch

chain.

$$\boldsymbol{\tau} = \sum_{i=1}^3 \left(\frac{d}{dt} \frac{\partial L}{\partial \dot{\mathbf{q}}} - \frac{\partial L}{\partial \mathbf{q}} - \sum \mathbf{J}_k^T \begin{bmatrix} \mathbf{F}_k \\ \mathbf{M}_k \end{bmatrix} \right)_{C_i} + \mathbf{T}(\mathbf{q}, \dot{\mathbf{q}}). \quad (3)$$

Since the branch chains C_1 and C_2 constitute loop A, and C_1 and C_3 constitute loop B, Eq. (3) can be written in the following form:

$$\boldsymbol{\tau} = \boldsymbol{\tau}|_{\text{loopA}} + \boldsymbol{\tau}|_{\text{loopB}} - \boldsymbol{\tau}|_{C_1} + \mathbf{T}(\mathbf{q}, \dot{\mathbf{q}}) \quad (4)$$

where $\boldsymbol{\tau}|_{\text{loopA}}$ is the actuator torque vector with all elements zero except for those of the open-loop chain A, i.e., from 1st to n th element. The vectors $\boldsymbol{\tau}|_{\text{loopB}}$ and $\boldsymbol{\tau}|_{C_1}$ are defined in a similar manner.

$$\boldsymbol{\tau}|_l = \left(\mathbf{M}(\mathbf{q})\ddot{\mathbf{q}} + \mathbf{V}(\mathbf{q}, \dot{\mathbf{q}}) + \sum_i \mathbf{J}_i^T m_i \mathbf{g} + \sum_k \mathbf{J}_k^T \begin{bmatrix} -\mathbf{F}_k \\ -\mathbf{M}_k \end{bmatrix} \right)_l \quad (l = \text{loopA}, \text{loopB}, C_1). \quad (5)$$

For dual-arm human motion, assume that the only generalized torque vector due to the joint internal characteristics is the restoring torque vector $\boldsymbol{\tau}^{\text{Restoring}}$ from the joint stiffness.

$$\mathbf{T}(\mathbf{q}, \dot{\mathbf{q}}) = -\boldsymbol{\tau}^{\text{Restoring}} = \mathbf{K}(\mathbf{q} - \mathbf{q}^N) \quad (6)$$

where \mathbf{K} is a diagonal stiffness matrix, and \mathbf{q}^N is the neutral joint variable vector.³⁵ Then the equations of motion for a human model subject to several external loads can be written as follows:

$$\boldsymbol{\tau} = \boldsymbol{\tau}|_{\text{loopA}} + \boldsymbol{\tau}|_{\text{loopB}} - \boldsymbol{\tau}|_{C_1} + \mathbf{K}(\mathbf{q} - \mathbf{q}^N). \quad (7)$$

3. Problem Definition and Optimization Formulation

The problem of motion planning for redundant systems is defined as follows: The inputs to the algorithm are the link parameters, dynamic parameters (such as mass, centers of mass, moments and products of inertia, joint stiffness, and damping coefficients), joint variable limits, actuator torque limits (possibly as functions of joint velocity), points of application and components of external loads, and task-specific constraints (such as the time desired to perform the task, end-effector path, and orientations). Then it is desired to generate the joint profiles that guarantee the execution of the task, where the external loads can have broad ranges of magnitudes. To resolve the redundancy, the problem is formulated as an optimization problem, where the outputs are the joint variable profiles, the required actuator torques, and the energy rates as functions of time. For human model, this is based on the assumption that humans naturally generate effective motion to accomplish a given task in such a way as to minimize certain cost function(s). The optimization variables are the control points of the joint B-spline curves of degree 3, which have many beneficial properties such as continuity, differentiability, endpoint interpolations, local control, and

convex hull.⁴² A total of 11 distinct knots are assigned and 13 control points are used for each joint.

It should be emphasized that the general external loads term, as well as the inertia and gravity, must be included in the calculation of actuator torques to guarantee the execution of the planned motion. Then the load-effective motions are the feasible motions where the general external loads are taken into account for the calculation of required actuator torques that are used for the constraints and/or the cost function. The energy consumption used as the cost function will result in the most efficient motion. The details of the energy consumption and constraints are described in the following sections.

Since the proposed methodology framework is based on optimization, the numerical performance and complexity of the proposed algorithm depend on the components and the specific techniques of optimization. Although the dynamic model (2) is included in the optimization components (cost function and constraint), its effect on the overall computational complexity is not significant. This is because the current formulation does not require integration or matrix inversion of the equations of motion. Thus, the overall numerical performance depends mainly on the optimization technique. We use the sequential quadratic programming (SQP) method that uses quasi-Newton approximations to the Hessian of the Lagrange function and obtains search directions from a sequence of quadratic programming sub-problems. The second-order information about the problem functions is approximated using first-order information only, and this provides the high rate of convergence of the algorithm because the curvature information for the functions is used in determining the search direction. SQP methods have been proved to be most efficient and reliable for solving large-scale constrained optimization problems with smooth nonlinear cost function and constraints.^{43,44} Thus the SQP method is suitable for the current problem that deals with the motions of highly articulated human model.

3.1. Energy consumption

Energy has a unifying property, into which the dynamic as well as the kinematic characteristics of motion are incorporated. The actual formula representing the energy consumption for a system varies depending on the specific properties of the system, as well as the types of actuators. Many simplified forms of the general energy consumption are widely used in literature. For human motion planning, the metabolic energy consumption from time t_1 to t_2 ³⁵ will be used as a cost function for the optimization problem.

$$E_{\text{Metabolic}} \approx \int_{t_1}^{t_2} \sum_{i=1}^n |\tau_i(t) \dot{q}_i(t)| dt + \int_{t_1}^{t_2} \sum_{i=1}^n h_m^i |\tau_i(t)| dt + \int_{t_1}^{t_2} \dot{B} dt \quad (8)$$

where $h_m^i (i = 1, \dots, n)$ are the coefficients of the generalized maintenance heat, and \dot{B} is the basal metabolic rate. The actuator torques are obtained from the equations of motion. It had been shown that h_m^i is inversely proportional to the maximum torque limit of joint i . Therefore, for small

joint velocities, the human motion of minimum energy (thus minimum weighted torques) implies that humans tend to use the stronger joints to accomplish a given task rather than the weaker ones. This means that the actuator torques are distributed so that the larger torques are exerted at the stronger joints and vice versa, which can be observed in real-world human tasks.

The use of energy consumption as a cost function implies several important points. Firstly, minimum energy consumption indicates minimum fuel usage. Secondly, for smooth movement of each joint, the magnitude of the second derivatives of the joint curves needs to be minimized to avoid an abrupt change in the joint velocity. Although minimum jerk has been used in literature as a stronger criterion (e.g., refs. [2, 45]), the second derivatives of the joint variables in the energy cost function provide a natural way to ensure the smooth movement of each joint by reducing unnecessary fluctuations in the joint curves. Finally, minimizing energy consumption implicitly indicates minimizing required actuator torques and joint stress.

3.2. Constraints

The following is a list of basic constraints that are typically given from the system properties and the task requirements. Depending on the task definition and the environment, various other constraints can be imposed in addition.

1. *Joint variable limits:* Each joint variable has bilateral constraints imposed in the form of

$$q_i^L \leq q_i \leq q_i^U \quad (i = 1, \dots, n) \quad (9)$$

where q_i^L and q_i^U are the lower and upper limits for each joint variable, respectively.

2. *Actuator torque limits:* The torque limit is usually a function of the joint velocity (even for real human), which is represented as a torque–speed curve of each actuator. The torque–speed curves depend on the class and capacity of the actuators.

$$\tau_i^L(\dot{q}_i(t)) \leq \tau_i \leq \tau_i^U(\dot{q}_i(t)) \quad (i = 1, \dots, n) \quad (10)$$

where τ_i^L and τ_i^U are the lower and upper limits, respectively, for each actuator torque. Generally, τ_i^L is negative and τ_i^U is positive.

3. *Position and orientation constraints:* The configuration of a rigid link of a system in space can be described uniquely by assigning it three independent position coordinates and three independent orientation angles. Depending on the task requirements, some of these six coordinates can be constrained, while the rest are left as free DOFs. For position constraints, the Cartesian coordinates of the point as a function of the joint variables are constrained. For orientation constraints, the direction of the unit vectors of the link local frame is constrained in terms of the global frame.

4. *Path constraints:* The end-effector path in Cartesian space may be either constrained by task requirements or naturally unconstrained. Usually, the path is given as task requirement. For example, the end-effector paths of drawing a straight line or welding on a surface are predetermined from the task requirements. Suppose the end-effector path for the

task is assigned as a parametric curve in Cartesian space such as

$$\mathbf{path}(t) = [x_{\text{path}}(t), y_{\text{path}}(t), z_{\text{path}}(t)]^T. \quad (11)$$

To ensure that the end-effector point characterized by $\mathbf{x} = [x, y, z]^T$ as a function of joint variables stays on the path during the motion, the distance from the end-effector point to the desired path in the Cartesian space is enforced as a constraint:

$$\|\mathbf{x}(\mathbf{q}(t)) - \mathbf{path}(t)\| \leq \varepsilon \quad (12)$$

where $0 \leq t \leq t_f$ and ε is a small positive number as a specified tolerance (e.g., 0.001).

4. Example Results and Discussion

The proposed formulation will be demonstrated using the highly articulated dual-arm human model with 30 DOFs. A computer with Intel[®] Xeon[™] 3.06 GHz processor is used for calculation. Each task is simulated for two different load magnitudes, and the time duration for the task is given as 2 s. Although simple tasks are illustrated as examples in this paper, the proposed method can be easily applied to more complicated tasks.

Lever-pulling: We consider the dual-arm motion of pulling a lever with constant load from a given initial position to a given final position. The initial position of the lever is (0, 19, 70) (cm), and the final position of the lever is (0, 19, 40) (cm) in the global coordinate frame where the path of the lever between the initial and final positions is given as a straight line. Two different pulling forces are tested: 1 N and 800 N. Figures 4–6 show the generated motions and calculated results of several notable joints for both cases (with run-time

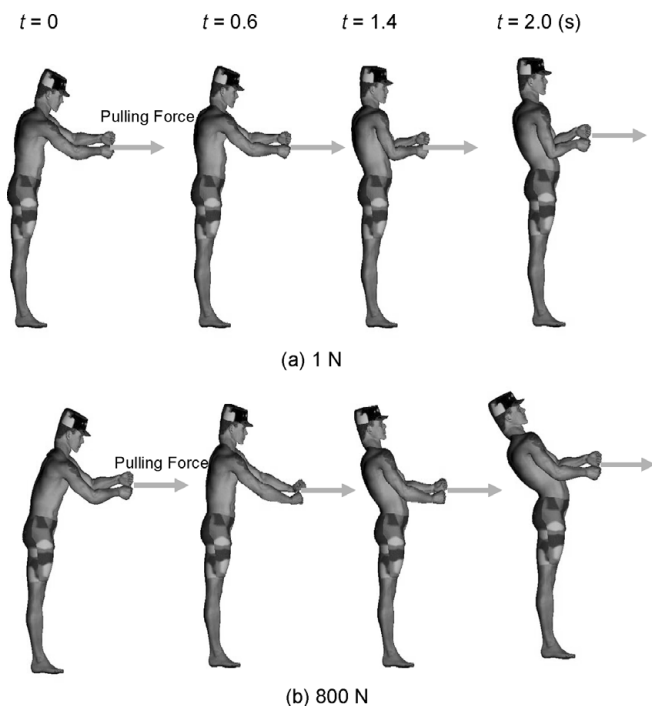


Fig. 4. Motions of dual-arm lever-pulling.

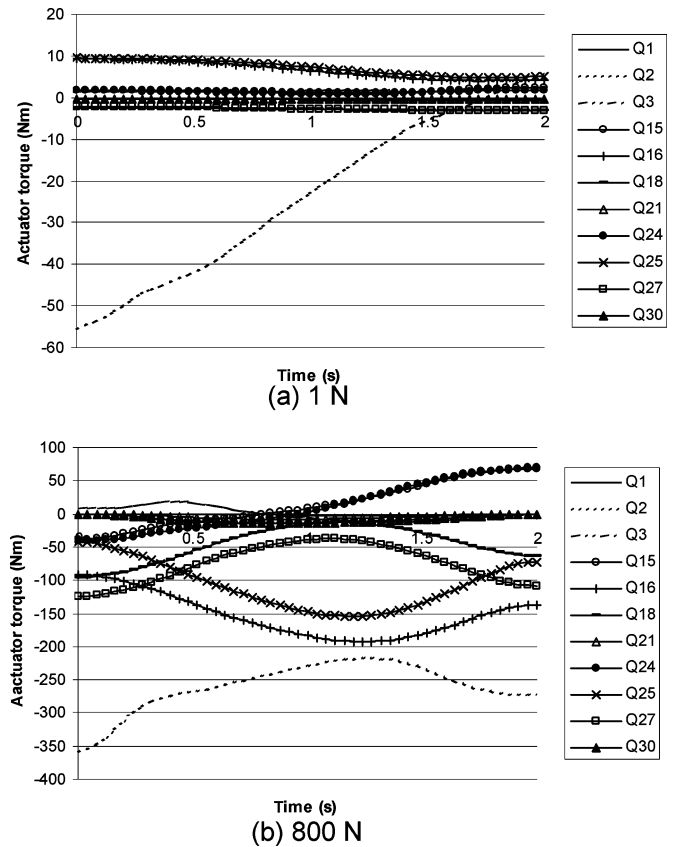


Fig. 5. Actuator torque profiles for dual-arm lever-pulling.

around 75 min and 265 major iterations). The total metabolic energy consumed for the 1-N lever-pulling is 301.21 J, and that for the 800-N lever-pulling is 1440.55 J. These values also represent how much effort is required to perform each task.

It is observed that the human model generates different motions for different magnitudes of external load. For the lever load of 1 N, the torso is almost vertical, while for the larger load of 800 N, the torso is extended backward to use its own body weight to counter-balance the large pulling load at both hands. In Fig. 5(b), the large negative actuator torque values for torso extension (joint 2) and shoulders (joints 16 and 25) for the 800-N lever-pulling indicate the major contributions of these joints to the pulling motion. These large actuator torques are used to generate the torso motion while sustaining the large pulling force in the forward direction. In this way, the human can also straighten both its arms in the final posture to minimize the actuator torques at the wrists and elbows.

Experimental measurements on the similar tasks of actual human subjects were reported in the literature,⁴⁶ where the effects of hand force magnitudes and direction on body postures have been studied. It has been observed that the subjects lean back (torso inclination) into the direction of pulling force. Their study shows similar features as our predicted motions, and serves as a partial validation of our calculated results. In fact, it is often observed in the real world that, when pulling or dragging a very heavy object, a human usually leans the body in the desired direction of pulling. In other words, to accomplish a given task,

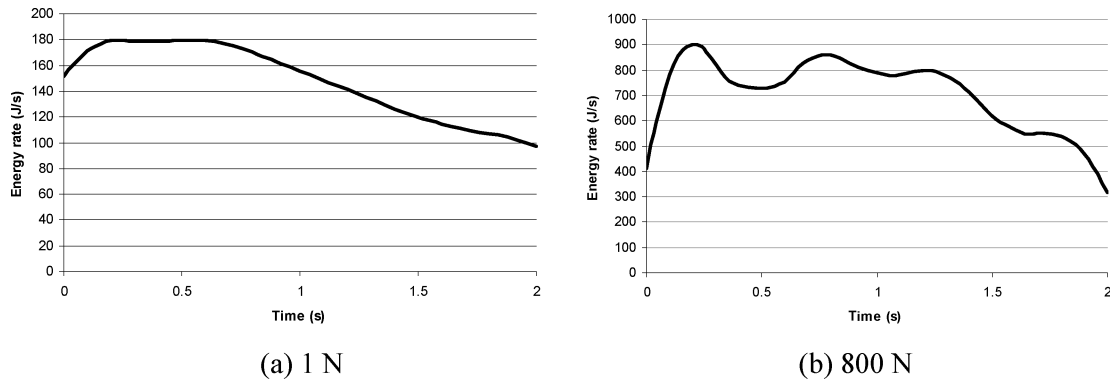


Fig. 6. Metabolic rate profiles for dual-arm lever-pulling.

humans naturally generate effective motion that minimizes the required actuator torques within the actuator capacities (torque limits). A similar argument can be made for the motion of pushing a heavy object, where it is frequently observed that a human leans the body in the direction of pushing.

Rope-pulling: The next task is to pull a rope using two hands with light (1 N) and heavy (100 N) weights. The rope is stretched toward the human’s right side. The initial positions of the right and left hands are (−60, 40, 20) (cm) and (−20, 40, 20) (cm), respectively, and the final positions are (−30, 40, 20) (cm) and (10, 40, 20) (cm), respectively, in the global Cartesian frame. The resulting motions, actuator torques, and metabolic rates for both cases are shown in Figs. 7–9. The computation time is around 23 min and the number of major iterations is 80.

The torso is tilted toward the left for the 100-N pulling, while it remains upright for the 1-N pulling. Again, this can be explained by analyzing the configuration at each time step. By bending its torso laterally toward the left, the human can use its own body weight to counter-balance the large force on its right side; it can thus reduce or

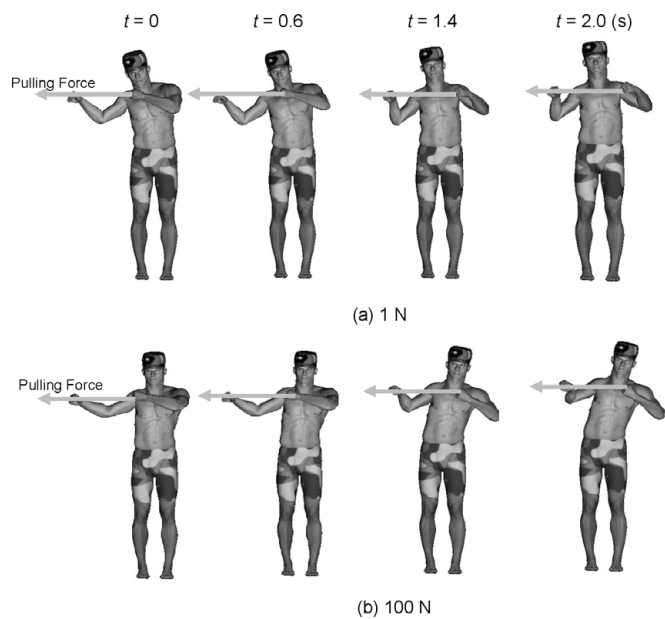


Fig. 7. Motions of dual-arm rope-pulling.

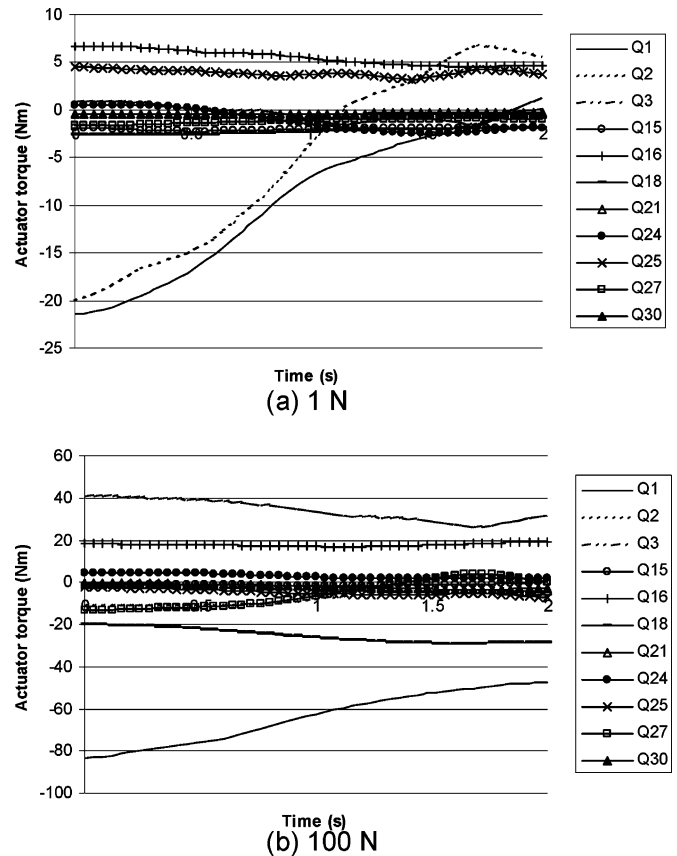


Fig. 8. Actuator torque profiles of dual-arm rope-pulling.

minimize the required actuator torques. The right arm for large-force pulling is nearly straight during the initial stage of the motion, while this is not notable in small-force pulling. For the large-force pulling, the left arm motion is generated such that the wrist and elbow joints are located as close as possible to the line of pulling-force application. This motion is generated in an effort to minimize the actuator torques and is usually observed in the real-world human motions for large-force pulling. It can be seen that the large actuator torque values for the torso left lateral bending (joint 1) and the torso left axial rotation (joint 3) in Fig. 8(b) are mainly used to sustain the large pulling force. The total metabolic energy consumption for the 1-N rope-pulling is 241.75 J, and that for 100 N is 516.41 J. Then the average energy consumption rate is $241.75 \text{ (J)}/2 \text{ (s)} = 120.87 \text{ (J/s)}$

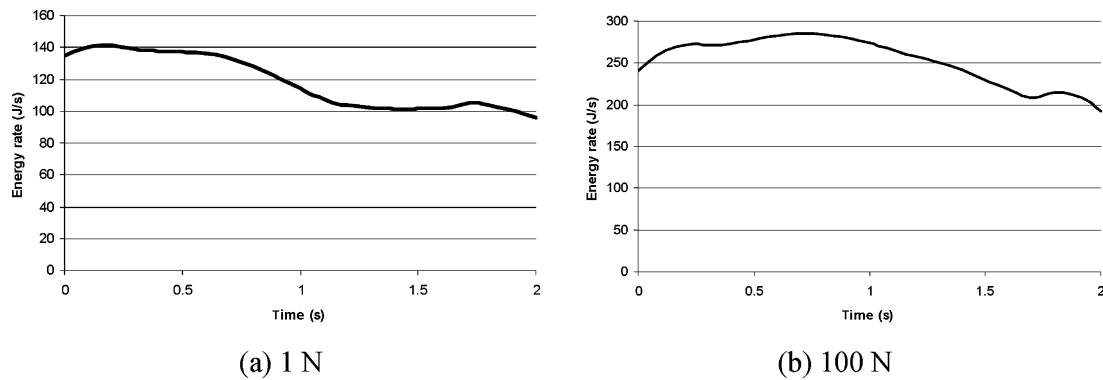


Fig. 9. Metabolic rate profiles of dual-arm rope-pulling.

and $516.41 \text{ (J)}/2 \text{ (s)} = 258.20 \text{ (J/s)}$, respectively, which are reasonable values for human activities. Again, the human model generated different effective motions for different magnitudes of external load.

5. Conclusions

In past motion planning problems, general external loads other than gravity were not considered extensively. In this paper, a method for planning load-effective dynamic motions for redundant systems, especially highly articulated human model, is proposed. A comprehensive form of the equations of motion for tree-structured systems is formulated in which the general external loads, as well as the inertia and gravity terms, are incorporated. The comprehensive dynamics model is then implemented into the constraints and/or the cost function of the optimal motion planning problem. The physics-based motions generated for tree-structured human model demonstrates different effective dual-arm human motions for different magnitudes of external load. The results provide a new scientific insight of natural human motion. Although the simulated features are validated in the literature, more rigorous quantitative experimental study for comparison is suggested as future research. Overall, the proposed optimization-based methodology is broadly applicable for any type of kinematic chain systems with general external loads.

Acknowledgments

This research is partially supported by the U.S. Army Tank Automotive Research, Development and Engineering Center and the U.S. Army Natick Soldier Systems Center.

References

1. L. Sciavicco and B. Siciliano, "A solution algorithm to the inverse kinematic problem for redundant manipulators," *IEEE J. Rob. Automat.* **4**(4), 403–410 (Aug. 1988).
2. A. Piazzoli and A. Visioli, "Global minimum-jerk trajectory planning of robot manipulators," *IEEE Trans. Indus. Elec.* **47**(1), 140–149 (Feb. 2000).
3. P. E. Nikravesh, *Computer-Aided Analysis of Mechanical Systems* (Prentice-Hall, Englewood Cliffs, New Jersey, 1988).
4. E. J. Haug, *Computer-Aided Kinematics and Dynamics of Mechanical Systems* (Allyn and Bacon, Boston, 1989).
5. A. Jain and G. Rodriguez, "Recursive flexible multibody system dynamics using spatial operators," *J. Guidance, Control Dyn.* **15**(6), 1453–1466 (1992).
6. S. K. Saha, "A decomposition of the manipulator inertia matrix," *IEEE Trans. Rob. Automat.* **13**(2), 301–304 (1997).
7. K. S. Anderson and S. Duan, "A hybrid parallelizable low order algorithm for dynamics of multi-rigid-body systems: Part I, chain systems," *J. Math. Comput. Model.* **30**, 193–215 (1999).
8. K. S. Anderson and S. Duan, "Highly parallelizable low order dynamics algorithm for complex multi-rigid-body systems," *AIAA J. Guidance, Control Dyn.* **23**(2), 355–364 (2000).
9. W. Blajer, "On the determination of joint reactions in multibody mechanisms," *J. Mech. Des.* **126**(2), 341–350 (Mar. 2004).
10. H. Hemami and B. F. Wyman, "Rigid body dynamics, constraints, and inverses," *J. Appl. Mech.* **74**(1), 47–56 (Jan. 2007).
11. K. Lee, Y. Wang and G. S. Chirikjian, "O(n) mass-matrix inversion for serial manipulators and polypeptide chains using Lie derivatives," *Robotica* **25**(6), 729–750 (2007).
12. K. Suh and J. Hollerbach, "Local Versus Global Torque Optimization of Redundant Manipulators," *Proceedings of IEEE International Conference on Robotics and Automation*, Raleigh, NC, USA, Vol. 4 (Mar. 1987) pp. 619–624.
13. R. S. Gompertz and D. C. H. Yang, "Feasibility Evaluation of Dynamically Linearized Kinematically Redundant Planar Manipulators," *Proceedings of IEEE International Conference on Robotics and Automation*, Philadelphia, PA, USA, Vol. 1 (Apr. 1988) pp. 178–182.
14. Y. Nakamura, *Advanced Robotics: Redundancy and Optimization*, Boston, MA, USA (Addison-Wesley, 1991).
15. A. Nedungadi and K. Kazeroonian, "A local solution with global characteristics for the joint torque optimization of a redundant manipulator," *J. Rob. Syst.* **6**(5), 631–654 (1989).
16. Y. S. Chung, M. Griffis and J. Duffy, "Unique joint displacement generation for redundant robotic systems," *ASME Rob., Spatial Mech. Mech. Syst.* **45**, 637–641 (1992).
17. C. Y. Chung, B. H. Lee, M. S. Kim and C. W. Lee, "Torque optimizing control with singularity-robustness for kinematically redundant robots," *J. Intell. Rob. Syst.* **28**(3), 231–258 (Jul. 2000).
18. Z. Shiller and S. Dubowsky, "On computing the global time-optimal motions of robotic manipulators in the presence of obstacles," *IEEE Trans. Rob. Automat.* **7**(6), 785–797 (Dec. 1991).
19. Z. Shiller, "Optimal robot motion planning and work-cell layout design," *Robotica* **15**(1), 31–40 (Jan. 1997).
20. S. K. Singh and M. C. Leu, "Manipulator motion planning in the presence of obstacles and dynamic constraints," *Int. J. Rob. Res.* **10**(2), 171–187 (1991).
21. C.-Y. E. Wang, W. K. Timoszyk and J. E. Bobrow, "Payload maximization for open chained manipulators: finding weightlifting motions for a Puma 762 robot," *IEEE Trans. Rob. Automat.* **17**(2), 218–224 (Apr. 2001).

22. S. F. P. Saramago and M. Ceccarelli, "An optimum robot path planning with payload constraints," *Robotica* **20**(4), 395–404 (2002).
23. J. E. Bobrow, F. C. Park and A. Sideris, "Recent Advances on the Algorithmic Optimization of Robot Motion," **In: Fast Motions in Biomechanics and Robotics**, Lecture Notes in Control and Information Sciences, Vol. 340 (Springer, Berlin/Heidelberg, 2006) pp. 21–41.
24. M. Vukobratovic and M. Kircanski, "A dynamic approach to nominal trajectory synthesis for redundant manipulators," *IEEE Trans. Syst., Man, Cybernet.* **SMC-14**, 580–586 (Jul.–Aug. 1984).
25. A. R. Hirakawa and A. Kawamura, "Trajectory generation for redundant manipulators under optimization of consumed electrical energy," *IEEE Industry Applications Conference, Thirty-First IAS Annual Meeting*, San Diego, CA, USA, Vol. 3 (Oct. 1996) pp. 1626–1632.
26. S. B. Nokleby and R. P. Podhorodeski, "Pose optimization of serial manipulators using knowledge of their velocity-degenerate (singular) configurations," *J. Rob. Syst.* **20**(5), 239–249 (Apr. 2003).
27. E. Papadopoulos and Y. Gonthier, "On Manipulator Posture Planning for Large Force Tasks," *Proceedings of IEEE International Conference on Robotics and Automation*, Nagoya, Japan, Vol. 1 (May 1995) pp. 126–131.
28. E. Papadopoulos and Y. Gonthier, "A framework for large-force task planning of mobile and redundant manipulators," *J. Rob. Syst.* **16**(3), 151–162 (Feb. 1999).
29. S. G. McLean, A. Su and A. J. van den Bogert, "Development and validation of a 3-D model to predict knee joint loading during dynamic movement," *J. Biomech. Eng.* **125**(6), 864–874 (2003).
30. W. Blajer and A. Czaplicki, "An alternative scheme for determination of joint reaction forces in human multibody models," *J. Theor. Appl. Mech.* **43**(4), 813–824 (2005).
31. M. Hirashima, K. Kudo and T. Ohtsuki, "A new non-orthogonal decomposition method to determine effective torques for three-dimensional joint rotation," *J. Biomech.* **40**(4), 871–882 (2007).
32. E. S. Jung, D. Kee and M. K. Chung, "Upper body reach posture prediction for ergonomic evaluation models," *Int. J. Indus. Ergonom.* **16**, 95–107 (1995).
33. K. Hase and N. Yamazaki, "Development of three-dimensional whole-body musculoskeletal model for various motion analyses," *JSME Int. J., Series C* **40**(1), 25–32 (Mar. 1997).
34. F. C. Anderson and M. G. Pandy, "Dynamic optimization of human walking," *J. Biomech. Eng.* **123**(5), 381–390 (2001).
35. J. H. Kim, K. Abdel-Malek, J. Yang and T. Marler, "Prediction and analysis of human motion dynamics performing various tasks," *Int. J. Human Factors Model. Simul.* **1**(1), 69–94 (2006).
36. H. Kawasaki, Y. Beniya and K. Kanzaki, "Minimum Dynamics Parameters of Tree Structure Robot Models," *Proceedings of IEEE International Conference on Industrial Electronics, Control and Instrumentation*, Kobe, Japan Vol. 2 (1991) pp. 1100–1105.
37. Y. Nakamura and K. Yamane, "Dynamics computation of structure-varying kinematic chains and its application to human figures," *IEEE Trans. Rob. Automat.* **16**(2), 124–134 (Apr. 2000).
38. J. E. Bobrow, B. Martin, G. Sohl, E. C. Wang, F. C. Park and J. Kim, "Optimal robot motions for physical criteria," *J. Rob. Syst.* **18**(12), 785–795 (Dec. 2001).
39. R. Featherstone and D. Orin, "Robot Dynamics: Equations and Algorithms," *Proceedings of IEEE International Conference on Robotics and Automation*, San Francisco, CA, USA, Vol. 1 (2000) pp. 826–834.
40. J. Denavit and R. S. Hartenberg, "A kinematic notation for lower-pair mechanisms based on matrices," *J. Appl. Mech.* **77**, 215–221 (1955).
41. K. S. Fu, R. C. Gonzalez and C. S. G. Lee, *Robotics: Control, Sensing, Vision, and Intelligence*, New York, NY, USA (McGraw-Hill, 1987).
42. V. B. Anand, *Computer Graphics and Geometric Modeling for Engineers* (John Wiley and Sons, New York, 1993).
43. J. S. Arora, *Introduction to Optimum Design* (McGraw-Hill, New York, 1989).
44. P. E. Gill, W. Murray and M. A. Saunders, "SNOPT: An SQP algorithm for large-scale constrained optimization," *SIAM J. Optim.* **12**, 979–1006 (2002).
45. J. Yang, J. H. Kim, E. Pena Pitarch and K. Abdel-Malek, "Optimal Trajectory Planning for Redundant Manipulators Based on Minimum Jerk," *ASME International Design Engineering Technical Conferences*, New York City, NY (Aug., 2008).
46. S. G. Hoffman, M. P. Reed and D. B. Chaffin, "Predicting Force-Exertion Postures from Task Variables," *Proceedings of SAE Digital Human Modeling for Design and Engineering*, Seattle, WA (Jun. 2007).